IDENTIFICATION AND CHARACTERIZATION OF REDOX SITES IN SUPRAMOLECULAR SYSTEMS AND THEIR RELEVANCE FOR THE DESIGN OF PHOTOACTIVE DEVICES. Ru(II)/C$_{60}$-BASED DONOR–ACCEPTOR DYADS

Maurizio CARANO[a], Paola CERONI[a], Michele MAGGINI[b1], Massimo MARCACCIO[a], Enzo MENNA[b], Francesco PAOLUCCI[a1,]*, Sergio ROFFIA[a2,]* and Gianfranco SCORRANO[b]

[a] *Dipartimento di Chimica "G. Ciamician", Università di Bologna, Via Selmi 2, 40126 Bologna, Italy; e-mail:* [1] *paolucci@ciam.unibo.it;* [2] *roffia@ciam.unibo.it*
[b] *Centro Meccanismi CNR, Dipartimento di Chimica Organica, Università di Padova, Via Marzolo 1, 35131 Padova, Italy; e-mail:* [1] *maggini@chor.unipd.it*

This work is dedicated to the memory of Professor Antonín A. Vlček. It concerns with the localization and characterization of redox sites in molecular and supramolecular systems, developed in the perspective of realizing devices capable of performing complex and useful functions. These topics were of extreme interest to Prof. Vlček's scientific activity, and he greatly contributed to their development.

Professor Vlček frequently visited the electrochemistry group at the Department of Chemistry "G. Ciamician" in Bologna. During his stays, a great and respectful friendship developed. Besides having been a great friend, Prof. Vlček was also a master to two of the authors (S. R. and F. P.). His suggestions, concerning both the experimental and interpretative aspects of our results in the field of coordination electrochemistry, have been invaluable. Particularly important were his indications for the improvement of the experimental conditions in our experiments, achieved by a very careful treatment of solvents and electrochemical cells. Regarding the theoretical aspects, the concept of redox sites developed by Prof. Vlček, their identification and characterization within the molecular and supramolecular framework, plays a fundamental role in obtaining important information regarding the possible occurrence, e.g., of intramolecular electron transfer processes, a theme that is central in our research.

We and all those who knew him will certainly be missing Prof. Vlček for many years to come.

Two dyads consisting of a mononuclear or a dinuclear ruthenium complex covalently linked to a fullerenopyrrolidine through a rigid androstane spacer, have been prepared through azomethine ylide cycloaddition to C$_{60}$. Electrochemical and photophysical studies revealed that ground-state electronic interactions between the dinuclear ruthenium chromophore and the fullerenopyrrolidine moiety are small. The redox series observed for the dyads correspond to the superimposition of the reduction patterns of the fullerene core and of the Ru(II)-bipyridine moieties. The results of the electrochemical investigation allow us to rationalize the photophysical behaviour of the two species by identifying the thermodynamically

allowed and forbidden routes for the deactivation of the Ru-based metal-to-ligand charge transfer (MLCT) excited state.

Polypyridine ruthenium(II) complexes have been extensively investigated in the past two decades because of their outstanding luminescence and electrochemical properties[1]. Their strong light absorption in the visible spectral region, well-known and highly stable photophysics, ability to undergo energy- and electron-transfer processes when coupled to electron acceptors, great chemical stability and relative ease of derivatization, make these species suitable building blocks for the development of molecular assemblies that may play an important role for many fundamental and practical aspects such as better understanding of natural photosynthesis and formation of molecular devices performing, for instance, information storage and processing or conversion of light into chemical/electric energy[2].

In the search for artificial photosynthetic systems based on the Ru(II)-polypyridine chromophore, [60]fullerenes have recently proved themselves as important electron acceptor units. This is related principally to their unique structure and electrochemical and photophysical properties. The good electron-accepting properties of fullerenes (in solution, they can accommodate up to six electrons and the first reduction occurs at remarkably high potentials[3]) couple to the low reorganization energy for the electron transfer (ET) process (essentially due to the rigidity of the bulky carbon sphere in the ground, reduced and excited states), resulting in the facilitated photoinduced ET process and inhibited back-ET (ref.[3a]). Finally, the high control reached in the chemical functionalization of fullerene[4] has made available a variety of approaches to the construction of donor-bridge-acceptor dyads based on a [60]fullerene unit opportunely coupled to suitable electron donors[5]. We have recently reported the case of the [Ru(bpy)$_3$]-androstane-fullerenopyrrolidine dyad **1** (Chart 1)[6], and a detailed characterization of its redox properties based on a comparison with those of its building blocks is reported in this work.

In the strategy of increasing the efficiency of such photochemical devices, by increasing the fraction of captured light through enhancing molar absorption coefficients in the visible region, and, hence, also the antenna effect, the dinuclear dyad **2** (Chart 1) was synthesized[7]. Its electrochemical characterization is given hereinafter, too.

The electrochemical characterization of the above species, in terms of (i) localization of the redox sites within the supramolecular structure and (ii) determination of the corresponding standard electrode potentials, as shown
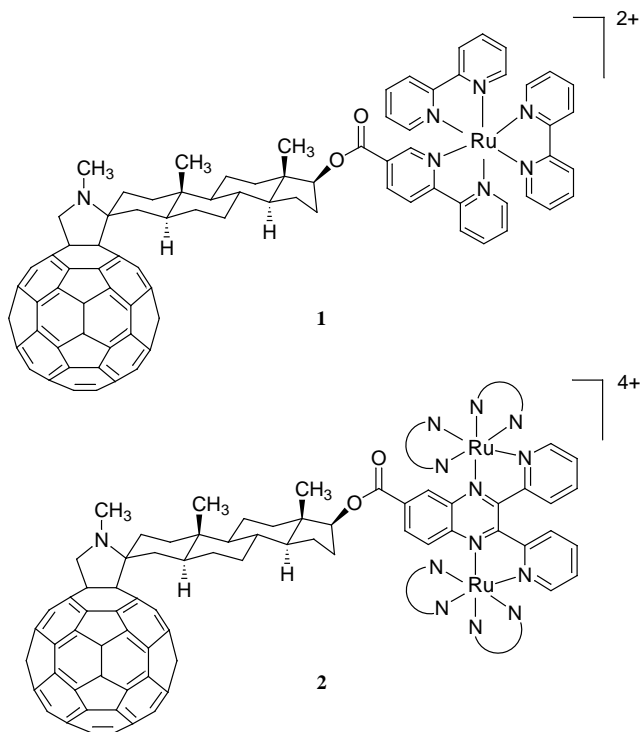

CHART 1

below, plays an instrumental role in the rationalization of the photophysical behaviour. The data obtained from the cyclic voltammetric (CV) experiments permit in fact the straightforward calculation of the intramolecular charge-separated state energy, which in turn sets the thermodynamic requirement for the ET process to occur.

RESULTS AND DISCUSSION

Localization of Redox Sites in Multicomponent Systems

A *redox site* is a domain of atoms within the molecular structure, over which the redox orbital is delocalized. The redox site concept is instrumental in

the definition of *redox series*, *i.e.* a set of compounds with identical chemical composition that only differ in the overall number of electrons. The redox series concept originated in the 1970s mainly in connection with the electrochemistry of coordination compounds[8], and was formalized by A. A. Vlček at the beginning of 1980s in a series of fundamental papers where the rules that govern, in particular, the pattern of ligand-based redox series, were laid[8]. A widespread diffusion of this concept in both the inorganic and organic electrochemical literature was then observed, mainly due to the fact that it has permitted a unified description and rationalization of the redox behaviour of families of complex systems in terms of localized redox processes, and, at the same time, the precise evaluation of the electronic interactions occurring between different redox sites. A molecule, and, *a fortiori* a supermolecule, may contain several redox orbitals that belong to different parts of space spanned by the molecule. In cyclic voltammetry, a redox series is manifested by a succession of reversible voltammetric peaks, and the separation between them is related to the interactions between the various sites. Coordination chemistry offers several examples that illustrate different types of redox series. In transition metal coordination compounds, it is usually possible to discriminate between metal-centred and ligand-centred redox series. Ligand–ligand interactions, occurring either through space or mediated by the metal core, are responsible for the potential separation usually observed between consecutive reductions of identical ligands in mononuclear complexes, and give rise to the typical multiplets observed in the CV patterns for such species. The complex $[Ru(bpy)_3]^{2+}$ (bpy = 2,2′-bipyridine) is a typical example of a coordination compound in which metal–ligand and ligand–ligand interactions are weak enough to secure that its reduction behaviour is easily related to that of the free ligands (Fig. 1).

The interaction with the metal stabilizes the bpy-centred redox orbital and, consequently, bpy is reduced at less negative potentials in the coordinated state than non-coordinated. Due to their chemical equivalence, the three ligands should reduce at the same potential but ligand–ligand interactions intervene, provoking their splitting in a triplet of peaks, one for each one-electron bpy reduction. The intramultiplet potential gaps reflect the electronic repulsion energy between electrons located on different ligands, while the intermultiplet potential gap relates to the electronic coupling energy of two electrons entering the same redox orbital, and, to a first approximation, is equal to that measured for the free ligand. It should be noted that polypyridine ligands are strong bases when doubly-reduced. This means that a symmetric, reversible pattern such as that shown in Fig. 1, can

only be obtained when very dry conditions are used in the CV experiments, otherwise follow-up protonation reactions bring about the early termination of the redox series, *i.e.* a smaller number of reduction peaks is observed, displaying a much lower reversibility. Extracting information on thermodynamical significance from the CV experiments is straightforward when a reversible behaviour is observed, whereas it may be done, in the case of kinetic complications[9], only by digital simulation procedures. The use of strictly aprotic conditions is therefore a convenient choice, although sometimes highly demanding from the experimental point of view[10].

More complex redox series than that shown in Fig. 1 may be observed, for instance, when the coordination compound contains different ligands with different redox properties, and also in polynuclear complexes. In the latter case, in addition to the above types of interactions, metal–metal interactions (direct or mediated by bridging ligands, the latter being either electroactive or not) and remote ligand–ligand interactions have also to be considered.

In this context, the supramolecular systems shown in Chart 1, in which the polypyridine Ru(II) complex and the fullerene moieties separately give rise to redox series, having different and partly superimposing patterns, represent interesting examples for illustrating and testing the above concepts. Moreover, the presence of either a mono- or a dinuclear metal complex allows to determine the different entity of the various types of interactions involving the ligands. Two different strategies for a satisfactory localization
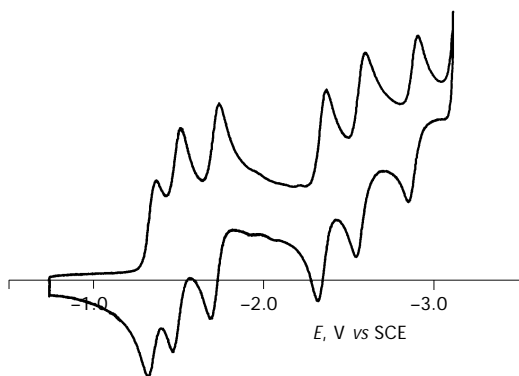

FIG. 1
Cyclic voltammogram of $[Ru(bpy)_3]^{2+}$ ($1 \cdot 10^{-3}$ mol l^{-1}) in DMF ($5 \cdot 10^{-2}$ M TEAH). Conditions: –54 °C, $v = 0.2$ V s^{-1}, working electrode: Pt wire

of redox sites will be illustrated, both based on the use of *genetic diagrams*, *i.e.* diagrams in which each redox potential for the various processes observed in the dyad, is correlated to that of an equivalent process observed in an appropriate model. In the case of the mononuclear dyad **1**, the correlation will involve the free ligands, and the effects on their redox properties deriving from complexation will be taken into account. On the other hand, in the case of the dinuclear dyad **2**, a correlation will be done with two suitable fragments, namely the fullerene derivative and the dinuclear Ru(II) complex, each responsible for one of the two redox series that superimpose in the CV pattern of the dyad.

Redox Sites Localization in Dyads *1* and *2*

Since the interaction between the two subunits in dyads **1** and **2** is expected to be weak, the cyclic voltammetric behaviour is discussed with the assumption that their ground state redox properties can be represented with a sufficient degree of approximation within the localized molecular orbital model.

Figure 2 shows the cyclic voltammogram of dyad **1** in THF. As expected for the presence of two subunits, each characterized by a rich redox activity, the curve shows a complex pattern made up of several one- and two-electron processes.
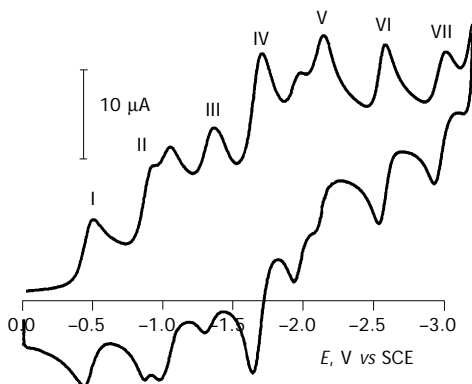

FIG. 2
Cyclic voltammogram of **1** ($3 \cdot 10^{-4}$ mol l^{-1}) in THF ($5 \cdot 10^{-2}$ M TBATFB). Conditions: 25 °C, v = 0.2 V s^{-1}, working electrode: Pt wire

The independence of the current function ($i/v^{1/2}$, where i is the current and v the scan rate) on the scan rate indicates that all the peaks correspond to reversible diffusion-controlled reduction steps. In particular, the first, third, sixth and seventh peaks correspond to a reversible one-electron transfer, while the second, fourth and fifth peaks are the result of superimposition of two successive reversible one-electron transfers with close standard potentials. In the whole, up to 10 electrons are exchanged reversibly, with $E_{1/2}$ values (reported in Table I) obtained for the one-electron peaks as a mean of E_{pa} and E_{pc}, and for the doublets by digital simulation of the CV curves.

In order to localize the redox sites within the supramolecular structure and to obtain information on their interactions, the cathodic voltammetric response for **1** was compared with that of the free ligands bpy and **3** (Chart 2). Furthermore, since ligand **3** is made up of two independent subunits, the *N*-methylfullerenopyrrolidine **4** and the substituted bpy fragment **5** (Chart 2), covalently linked by the electro-inactive androstane bridge, its CV behaviour is expected to be superimposition of those for separate subunits, with
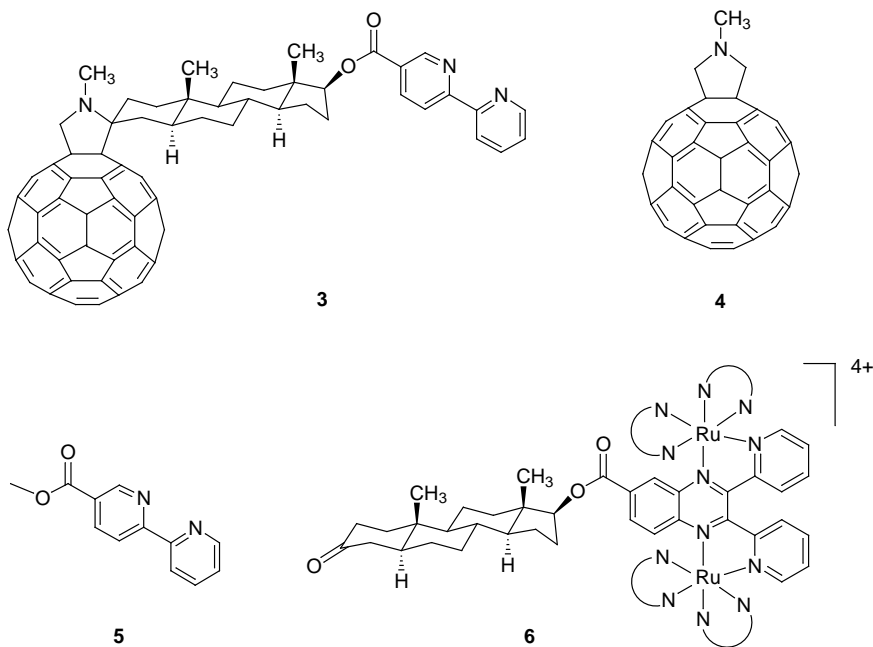

CHART 2

small changes due to weak interactions between them. Figure 3 shows the CV curves for **4** (a), **5** (b) and **3** (c) in THF solution at –60 °C, where a higher reversibility for all the processes was obtained.

All compounds show one-electron processes, except for the third and fourth peaks in **3**, each corresponding to two consecutive reversible one-electron transfers with close standard potentials (determined by digital simulation of the CV curve). The comparison of the CV curves in Fig. 3 allows the facile location of the redox sites in the ligand **3**. This is illustrated in the genetic diagram in Fig. 4, where the $E_{1/2}$ values for all the one-electron reduction processes involving species **3**–**5** (Table I), are displayed and the localization of the redox sites is shown by the one-to-one correlation lines.

Note that the spacing between the two reduction steps in **5** is the expected electronic coupling interaction term usually observed in polypyridine ligands, a separation that is usually conserved after complexation with the metal. Moreover, both reductions are positively shifted with respect to the corresponding processes in unsubstituted bpy (by 450 and 600 mV for the first and second reduction, respectively, *cf.* Table I). This is due to the presence of the electron-withdrawing carboxylic group in **5**. On the other hand, the slight negative shift of the last two fullerene-centred reductions in **3** is likely due to the electrostatic interaction between the fullerene moiety and the (reduced) bpy, although some electronic interac-

TABLE I
Half-wave potentials ($E_{1/2}$ *vs* SCE) for dyads **1** and **2** and their building blocks **3**, **4**, **5** and **6** and uncoordinated bpy in THF at 25 °C

Com-pound	Cathodic steps uncoordinated									
1	–0.47	–0.92	–1.04	–1.35	–1.69	–1.71	–1.95	–2.15	–2.56	–2.97
2	–0.23[a]	–0.55	–0.90[a]	–1.10	–1.52[b,c]	–1.71	–1.83	–1.95	–2.23	–2.73[b,c]
3	–0.47	–1.04	–1.68	–1.71	–2.18	–2.23	–2.96			
4	–0.47	–1.04	–1.68	–2.15	–2.96					
5	–1.71	–2.19								
6	–0.23	–0.91	–1.41	–1.50	–1.81	–1.97	–2.26	–2.65[b,c]		
bpy[d]	–2.16	–2.79								

[a] Adsorption phenomena. [b] Irreversible peak. [c] Two-electron process. [d] Ref.[9].
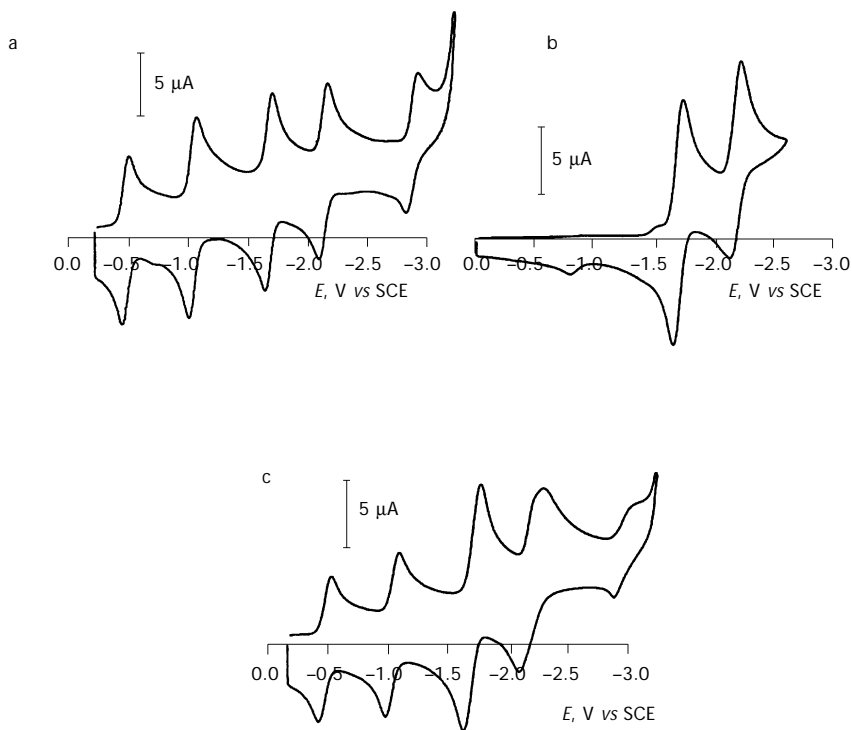
FIG. 3
Cyclic voltammograms of a **4**, b **5** and c **3** ($5 \cdot 10^{-4}$ mol l^{-1}) in THF ($5 \cdot 10^{-2}$ M TBATFB). Conditions: –60 °C, v = 0.2 V s^{-1}, working electrode: Pt wire
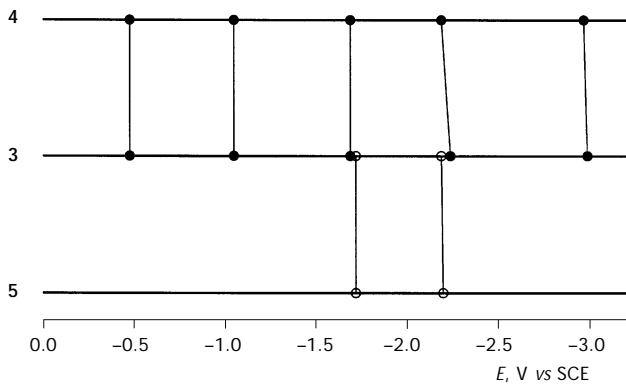

FIG. 4
Comparison of $E_{1/2}$ values (genetic diagram) for compounds **3**–**5**

tion through the bridge cannot be ruled out entirely. Knowing the location of the redox sites in **3**, we can now identify the redox sites in dyad **1**. A comparison of the reduction potentials of **1** and the uncoordinated ligands can be made through the genetic diagram in Fig. 5, where the lines correlate reduction processes involving the same ligand in either its free or coordinated state.

The genetic diagram has been constructed considering, on the one hand, the well-known stabilization of bpy-centred redox orbitals upon metal coordination, and, on the other hand, the fact that no substantial potential shift of the fullerene-centred reductions is expected upon coordination to the metal centre. Additional factors, whose effect on the CV pattern has been taken into account, are: (i) the different redox properties of the bpy moiety in ligand **3** with respect to unsubstituted bpy (see Table I) and (ii) the generation of doublets for the reductions of the two equivalent bpy ligands, according to the rules outlined in the previous section. The localization of bpy-centred reduction processes was obtained by analogy with similar heteroleptic polypyridyl Ru(II) complexes, such as $[Ru(dpp)(bpy)_2]^{2+}$ (dpp = 2,3- or 2,5-di(2-pyridyl)pyrazine)[10b], where the dpp ligand, similarly to the ester substituted bpy moiety in **3**, is easier to reduce than bpy. According to the genetic diagram in Fig. 5, the first bpy-centred reduction in **1** involves the substituted ligand, followed by two reductions involving the two unsubstituted bpy ligands. The successive three bpy-centred electrons would enter in the same sequence of coupling to the first set in the respective redox orbitals. However, only five processes attributed to the bpy ligands are observed, *i.e.* the redox series is not complete: a reduction step due
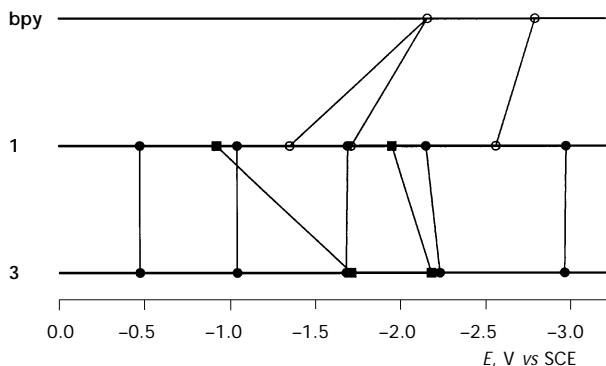

Fig. 5
Comparison of $E_{1/2}$ values (genetic diagram) for 2,2′-bipyridine, and compounds **1** and **3**

to one unsubstituted bpy is missing, occurring likely outside the available cathodic potential window. Note, moreover, that the assignment of the two closely-spaced processes comprised in the fourth and fifth peaks, as reported in the genetic diagram in Fig. 5, is only tentative and that the sequence may be reversed.

A different approach for the localization of redox sites was used for dyad **2**. Assuming that it contains two distinct redox-active sites, namely a fullerenopyrrolidine and dinuclear Ru(II) moieties, interacting in principle only weakly, the analysis of the CV response of **2** was based on that of the two separate models **6** and the fullerenopyrrolidine **3**. Seven distinct reduction peaks are observed for species **6** (Fig. 6). Peaks I, II, IV–VI correspond to chemically reversible one-electron reductions, whose $E_{1/2}$ potentials were directly measured (Table I). In contrast, peak III presents the overlap of two reversible one-electron processes, whose $E_{1/2}$ potentials could only be obtained by digital simulation of the CV curves. Finally, the multi-electron peak VII corresponds to the exchange of at least two electrons. Reversibility in the latter case is difficult to ascertain due to the poor resolution of the peak.

Based on the hypothesis that two electrons are exchanged at peak VII, the digital simulation provides the corresponding $E_{1/2}$ values reported in Table I. In analogy to electrochemical properties of similar bipyridine-type Ru(II) complexes containing pyrazine ligands[10a], with the bridging ligand
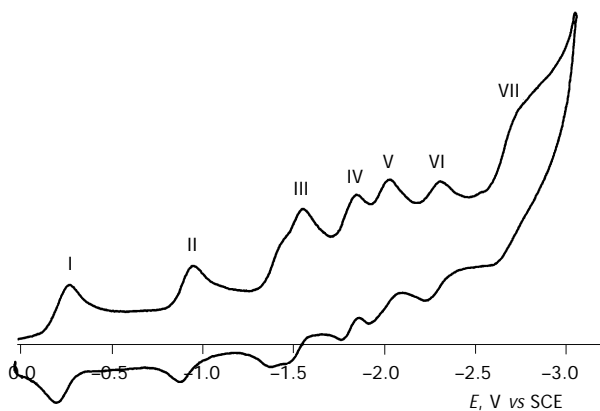

Fig. 6
Cyclic voltammogram of **6** ($5 \cdot 10^{-4}$ mol l^{-1}) in THF ($5 \cdot 10^{-2}$ M TBATFB). Conditions: 25 °C, v = 0.5 V s^{-1}, working electrode: Pt wire

reducing much easier than bpy and its double chelation making the reduction even easier, the peaks I, II and VI are assigned to the three consecutive reductions of the dpq bridging ligand. The two overlapping waves in the composed peak III, as well as the peaks IV and V belong to the one-electron reductions of the four bipyridine ligands. Finally, the two processes comprised in the peak VII correspond to the second reduction of two bpy units. The remaining bpy-centred reductions are not observed, being probably located outside of the available potential window. In line with the above attribution, the splitting between the processes hidden in the peak III and that between the peaks IV and V are those expected for the interaction between equivalent bpy ligands in dinuclear complexes[10a,10b]. Moreover, the dpq-centred reductions are anodically shifted (by *ca* 150–200 mV) with respect to those reported for the dinuclear Ru complex containing the unsubstituted dpq ligand[2f], as expected for the electron-withdrawing effect due to the carboxylic substituent.

The CV investigation of dyad **2** was difficult due to its very low solubility in THF or acetonitrile and by the occurrence of adsorption processes, evidenced by the presence of triangular-shaped peaks whose height increased linearly with the scan rate. The partial superimposition of such peaks to those due to the diffusion-controlled reductions of **2**, made the analysis of the CV curve, in particular the evaluation of the number of transferred electrons in the multi-electron reductions, rather tricky. Furthermore, the study proved a rather low stability of **2** upon multiple reduction, as evidenced on the reverse scan by the absence of the anodic counterpeaks for some of the cathodic steps and by the presence of novel anodic peaks not coupled to any of the cathodic ones. However, a tentative description of the redox
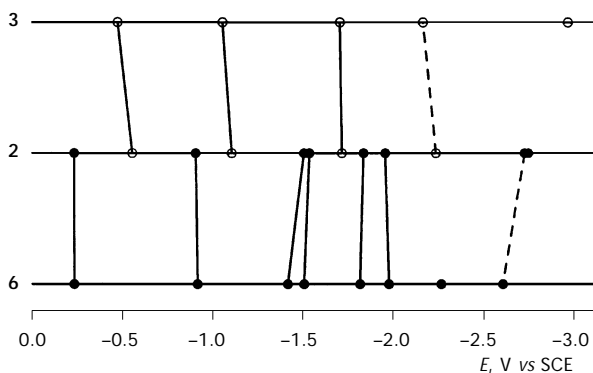

FIG. 7
Comparison of $E_{1/2}$ values (genetic diagram) for compounds **2**, **3** and **6**

properties of **2** is schematically shown in Fig. 7, based on a comparison of its CV pattern with those for models **6** and **3**. For all the reasons outlined above, a reliable localization of the redox sites in **2** cannot be obtained for all the redox processes.

Summarizing, the CV study has evidenced that, in contrast to the mononuclear dyad **1**, the first reduction is a ligand (dpq)-centred rather than a fullerene-centred process. In particular, the first reduction involving the fullerene moiety is located 320 mV towards more negative potentials.

Both dyads **1** and **2** show a significant quenching of the Ru-based ^{3}MLCT excited state emission with respect to the corresponding models that do not contain the fullerene moiety[6,7]. In principle, the quenching may occur either (i) *via* an energy transfer process to the C_{60} triplet excited state ($^3C_{60}$) or (ii) *via* the intramolecular ET from the excited complex to the good electron-accepting fullerene. Both mechanisms are subject to the thermodynamic requirement that the resulting state be exoergonic with respect to the Ru-based excited state. In view of the low energy of the $^3C_{60}$ excited state (1.50 eV), the mechanism (i) is thermodynamically allowed for both **1** (E_{00} = 1.97 eV)[6] and **2** (E_{00} = 1.75 eV)[7]. On the other hand, the driving force for the process (ii) may be calculated from electrochemical and spectroscopic (emission) data by using the equation: $-\Delta G_{ET} = E_{0-0} - e(E_D^0 - E_A^0) - \Delta G_s$, where E_{0-0} is the zero-level energy of Ru-based excited state, estimated from the emission data, E_D^0 and E_A^0 are the standard potentials for oxidation of the donor and reduction of the acceptor, respectively, and ΔG_s is the correction term for the effects of ion–solvent interaction in the charge separated (D$^+$–A$^-$) species, usually evaluated within the Born model[11]. On the basis of the electrochemical data collected in Table I and of emission data for **1** and **2**, ET is therefore thermodynamically allowed for **1** ($-\Delta G_{ET}$ = 0.24 eV in acetonitrile) while it is a forbidden process in **2** ($-\Delta G_{ET}$ = –0.17 eV in acetonitrile). In line with these results, time-resolved photolytic experiments showed the formation of the species $^3C_{60}$ and Ru(III)–C$_{60}^-$ upon the excitation of **1** (ref.[6]), while for **2**, only $^3C_{60}$ was detected[7].

CONCLUSIONS

Identification of the redox sites for the dyads **1** and **2** has been successful on the basis of a comparison with model molecules, and by the application of the rules developed within the redox series model; although, some ambiguity arises in the identification of redox processes occurring at very close potentials. The redox patterns for dyads **1** and **2** correspond to superimposition of those for the fullerene core and the Ru(II)-bipyridine moieties.

The results of the electrochemical investigation permitted to rationalize the photophysical behaviour of the two species by identifying the thermodynamically allowed and forbidden routes for the deactivation of the Ru-based MLCT excited state.

EXPERIMENTAL

Electrochemical Instrumentation and Measurements

The airtight single-compartment electrochemical cell was equipped with high-vacuum glass stopcocks fitted with either Teflon or Kalrez (DuPont) O-rings in order to prevent contamination by grease. Connections to a high-vacuum line and to the Schlenk flash containing the solvent were made by spherical joints fitted again with Kalrez O-rings. The pressure measured in the electrochemical cell *prior* to performing the trap-to-trap distillation of the solvent was typically 1.0–2.0 mPa. The working electrode was either a 0.6 mm-diameter platinum wire (*ca* 0.15 cm^2 active surface) sealed in glass, or a Pt disc ultramicroelectrode (r = 5 μm) also sealed in glass. The counter electrode was a platinum spiral and a silver coil served as the pseudo-reference electrode. The pseudo-reference electrode drift was negligible for the time required by a single experiment. Both the counter and reference electrodes were separated from the working electrode by *ca* 0.5 cm. Potentials measured with the internal ferrocene standard are always referred to saturated calomel electrode (SCE). In some experiments a SCE reference electrode was used, separated from the working electrode compartment by a sintered glass frit. Ferrocene was also used as an internal standard for confirming the electrochemical reversibility of a redox couple. Voltammograms were recorded with an AMEL Model 552 potentiostat or a custom-made fast potentiostat controlled by either an AMEL Model 568 function generator or an ELCHEMA Model FG-206F. The data acquisition was performed with a Nicolet Model 3091 digital oscilloscope interfaced to a PC. Temperature control within 0.1 °C was accomplished with a Lauda Klein-Kryomat thermostat. The DigiSim 2.1 software by Bioanalytical Systems Inc. was used for simulation of CV curves.

Materials

Compounds **1**–**6** were synthesized by procedures described elsewhere[6,7]. The supporting electrolytes tetrabutylammonium tetrafluoroborate (TBATFB, Fluka) or tetraethylammonium hexafluorophosphate (TEAH, Fluka) were used as received. Dimethylformamide (DMF, Merck) and tetrahydrofuran (THF, Merck) of spectroscopic quality were treated by procedures reported elsewhere[10]. For electrochemical experiments, the solvents were distilled *prior* to use into the electrochemical cell, using a trap-to-trap procedure[10].

REFERENCES AND NOTES

1. a) Yersin H., Vogler A. (Eds): *Photochemistry and Photophysics of Coordination Compounds*. Springer, Berlin 1987; b) Kalyanasundaram K. (Ed.): *Photochemistry of Polypyridine and Porphyrin Complexes*. Academic Press, London 1991; c) Horvath O., Stevenson K. L. (Eds): *Charge Transfer Photochemistry*. VCH, Weinheim 1993.

2. a) Juris A., Balzani V., Barigelletti F., Campagna S., Belser P., von Zelewsky A.: *Coord. Chem. Rev.* **1988**, *84*, 85; b) Collin J. P., Guillerez S., Sauvage J. P., Barigelletti F., Flamigni L., De Cola L., Balzani V.: *Coord. Chem. Rev.* **1991**, *111*, 291; c) Balzani V., Scandola F. (Eds): *Supramolecular Photochemistry*. Horwood, Chichester 1991; d) Balzani V., Juris A., Venturi M., Campagna S., Serroni S.: *Chem. Rev.* **1996**, *96*, 759; e) Ward M. D.: *Int. J. Photoen.* **1999**, *1*, 1; f) Belser P., Bernhard S., Blum C., Beyeler A., De Cola L., Balzani V.: *Coord. Chem. Rev.* **1999**, *192*, 155.

3. a) Guldi D. M.: *Chem. Commun.* **2000**, 321; b) Echegoyen L., Echegoyen L. E.: *Acc. Chem. Res.* **1998**, *31*, 593; c) Reed C. A., Bolskar R. D.: *Chem. Rev.* **2000**, *100*, 1075.

4. a) Diederich F., Thilgen C.: *Science* **1996**, *271*, 317; b) Prato M., Maggini M.: *Acc. Chem. Res.* **1998**, *31*, 519; c) Hirsch A. (Ed.): *Fullerenes and Related Structures*. Top. Curr. Chem., Vol. 199. Springer, Berlin 1999; d) Kadish K. (Ed.): *Fullerenes: Chemistry, Physics and Technology*. John Wiley & Sons, New York 2000.

5. a) Prato M.: *J. Mater. Chem.* **1997**, *7*, 1097; b) Imahori H., Sakata Y.: *Adv. Mater.* **1997**, *9*, 537; c) Martín N., Sánchez L., Llescas B., Pérez I.: *Chem. Rev.* **1998**, *98*, 2527; d) Imahori H., Sakata Y.: *Eur. J. Org. Chem.* **1999**, 2445; e) Diederich F., Gomez-Lopez M.: *Chem. Soc. Rev.* **1999**, *28*, 263.

6. Maggini M., Guldi D. M., Mondini S., Scorrano G., Paolucci F., Ceroni P., Roffia S.: *Chem. Eur. J.* **1998**, *4*, 1992.

7. Roffia S. *et al.*: Unpublished results.

8. a) Vlček A. A.: *Rev. Chim. Miner.* **1983**, *20*, 612; and references therein; b) Vlček A. A.: *Coord. Chem. Rev.* **1982**, *43*, 39; and references therein.

9. Krejčík M., Vlček A. A.: *J. Electroanal. Chem.* **1991**, *313*, 243. In A. A. Vlček's words: "The presence of an uncontrolled amount of water is obviously the main reason for large discrepancies in the literature both on the reversibility of the processes and on the values of the corresponding half-wave potentials". The procedures adopted in our laboratory, based on the chemical pretreatment of the solvents and on the use of high-vacuum techniques for the preparation of the electrochemical experiments, have allowed us to observe the largest redox series so far reported in the field of electro-chemistry of coordination compounds and fullerenes[10]. These procedures were introduced in our laboratory in the early 1980s, also thanks to the interaction with the late A. A. Vlček and his group in Prague.

10. a) Marcaccio M., Paolucci F., Paradisi C., Roffia S., Fontanesi C., Yellowlees L. J., Serroni S., Campagna S., Denti G., Balzani V.: *J. Am. Chem. Soc.* **1999**, *121*, 10081; b) Roffia S., Marcaccio M., Paradisi C., Paolucci F., Balzani V., Denti G., Serroni S., Campagna S.: *Inorg. Chem.* **1993**, *32*, 3003; c) Carano M., Ceroni P., Mottier L., Paolucci F., Roffia S.: *J. Electrochem. Soc.* **1999**, *146*, 3357.

11. a) Weller A.: *Z. Phys. Chem.* **1982**, *132*, 93; b) Gaines G. L. I., O'Neil M. P., Svec W. A., Niemczyk M. P., Wasielewski M. R.: *J. Am. Chem. Soc.* **1991**, *113*, 719.